2008-01-2072

# euces Software Development

**Armin Isselhorst, Nico Rackemann**
Thermal & Functional Propulsion Engineering, TE52
EADS Astrium GmbH, P.O. Box 286156, 28361 Bremen, Germany



## ABSTRACT

The euces project was initiated to be prepared for the future role of EADS as stage system prime for stage and launcher developments. Launcher stages for NGLV need to meet ambitious mission and operational demands. The paper will present a brief overview of the currently existing COMPONENT libraries and its possibilities as well as an application example which will be a simplified functional model of the ARIANE 5 EPS upper stage w.r.t. physical model formulation of its incorporated components, its schematic, data initialisation and simulation results obtained. The simulation results will be compared to flight data of a dedicated flight.

## INTRODUCTION

euces S/W development is an EADS Astrium *internal initiative* specifically dedicated to the development of launcher system and stage analysis software for the simulation of functional behaviour of launcher stages during its ground and flight phases. It incorporates the time-dependent simulation of the complete propulsion system including all its interacting components. In more detail, it comprises the evaluation of pressurant and propellant consumption, mass flows in the piping system, pressure regulation, feed-line chill-down in case of cryogenic propellants, engine characteristic parameters, ignitions and shut-down of engine and the sequence evaluation for the main propulsion or attitude control system. The categories involved are heat and mass transfer, thermodynamics, hydraulics, pneumatics, phase change of propellants, combustion, control and thermal aspects, as well as specific component design for tanks, valves, regulators, turbo machinery and rocket engines as a central role.

For the relevant hardware component formulation the existing hardware design of Ariane 5 upper stages was taken into consideration i.e. all hardware components have to be mathematically modelled adequately having an impact on the system simulation results.

euces will be based on EcosimPro kernel which was initially an ESA funded S/W tool developed by EAI for dynamic modelling and simulation for networks incorporating fluid flow (gaseous and liquid), heat and mass transfer, chemical reactions, controls, etc) providing a user-friendly simulation environment for modelling simple and complex physical processes. It provides an object-oriented approach towards creating reusable component libraries and expresses the system behaviour in terms of differential-algebraic equations and discrete events. The COMPONENTs will be linked via PORTs together to a complete system. PORTs are needed to exchange interconnection information between COMPONENTs as e.g. pressure, temperature or mass flow rate.

## 1. COMPONENT LIBRARY DEVELOPMENT

The objective of the euces project is the development of object-oriented S/W using EcosimPro kernel for functional physical model formulations and simulation of space propulsion H/W components and systems. The project tasks are linked to:

- tanks of known geometric configuration under 1g liquid level position
- pneumatic pipe system elements
- hydraulic pipe system elements
- engine system elements
- agglomeration in Libraries
- generation of simulation models of dedicated sub-systems
- generation of simulation models of dedicated propulsion systems
- comparison to ground/flight measurements

The actual component LIBRARIES in "workspace" euces and their main content are briefly presented for the different libraries.

AUXILLARY:

- global constants, complementary CONTROL (EAI) components, port definitions, complementary mathematical functions

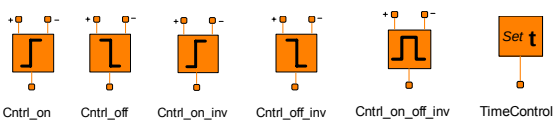

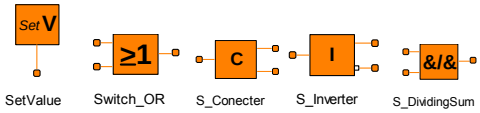


Mathematical functions have been implemented for solving quadratic and cubic equation, for linear curve and plane interpolation, for calculation of grid cover matrixes for static and moving grids.

SOLID_PROPERTIES:

- Titan, Carbon, AL2219, H920A, Dacron filled with He, Dacron filled with $N_2$, Cryosof, AL7020, stainless steel

The solid properties considered are density $\rho$, heat conductivity $\lambda$, specific heat capacity c partly in dependence of temperature T.

FLUID_PROPERTIES:

- Air, $H_2$, He, MMH, $N_2H_4$, $N_2$, $N_2O_4$, $O_2$, $H_2O$, R123, HFE7000

The fluid properties considered are for *ideal* gas and liquid phase density $\rho$, saturation pressure $p_s$, saturation temperature $T_s$, specific isobaric/isochoric heat capacity $c_p/c_v$, specific enthalpy h, specific internal energy u, isothermal compressibility $\kappa$, volume expansivity $\beta$, isochoric tension coefficient $\gamma$, heat conductivity $\lambda$, dynamic viscosity $\eta$, surface tension $\sigma$. In case of He also a real gas factor Z is considered as well as a pressure dependence for the specific enthalpy h.

GAS_TANKS:

- gas part: 1 or 2 gasses, 0 or 1D discretized
- spherical tank wall: heat conduction 1D radially discretized
- internal heat transfer functions

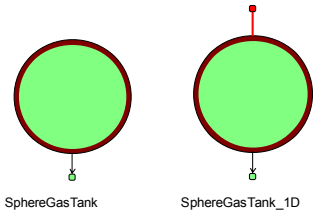


PROP_TANKS:

- ullage part: 2 gasses, 1 gas in PORT
- liquid part: pure liquid or 2-phase
- moving liquid level with surface calculation
- internal heat and mass transfer functions
- different tank shapes
- tank wall 0D heat conduction separated for gas/liquid part
- time-dependent external heat load or temperature separated for ullage and liquid part

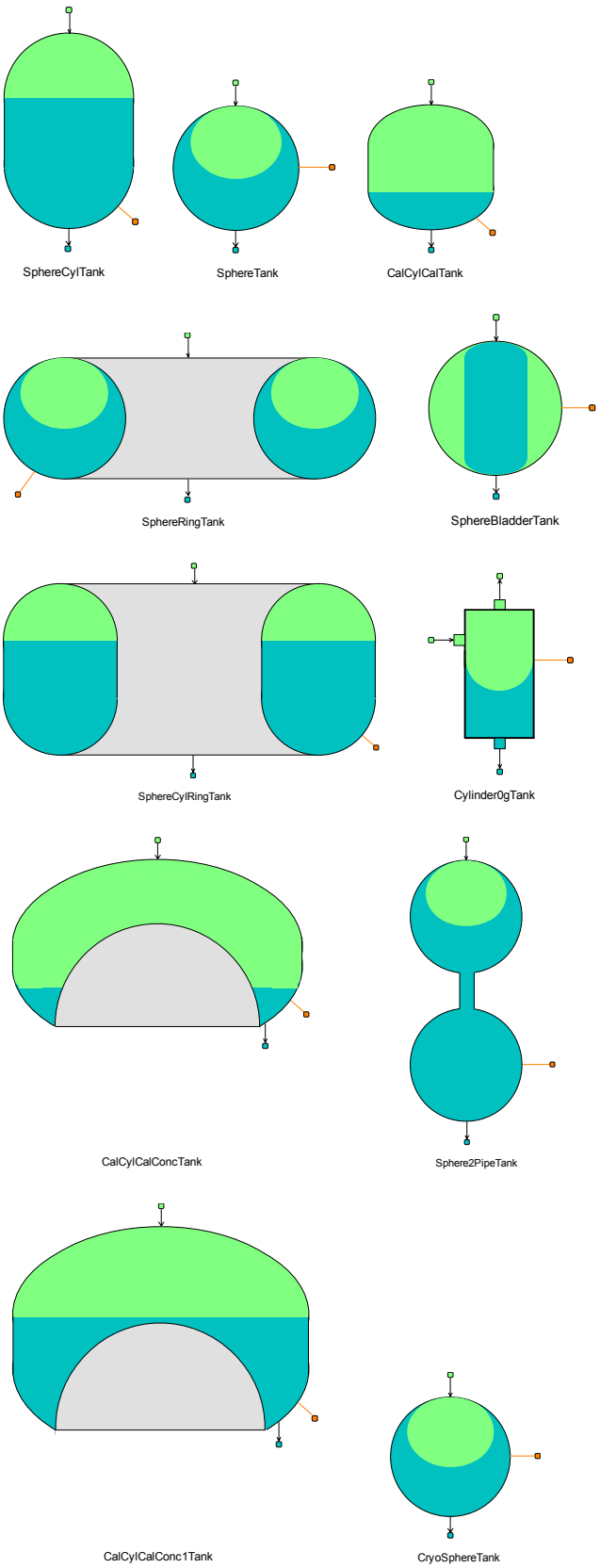


HYDRAULIK

- liquid components, only forward flow
- pipes (RC) and volumes (C) include fluid volume with thermodynamic properties and consideration of wall and flow calculation

- divider/combiner (RC) include fluid volume with thermodynamic properties and flow calculation
- valves, orifice, bust disc, filter (R) consider flow calculation
- hot gas thrusters (R) consider flow calculation, performance is modelled incl. test adjustments
- check valve consider force balance at poppet and flow calculation in dependence of poppet position

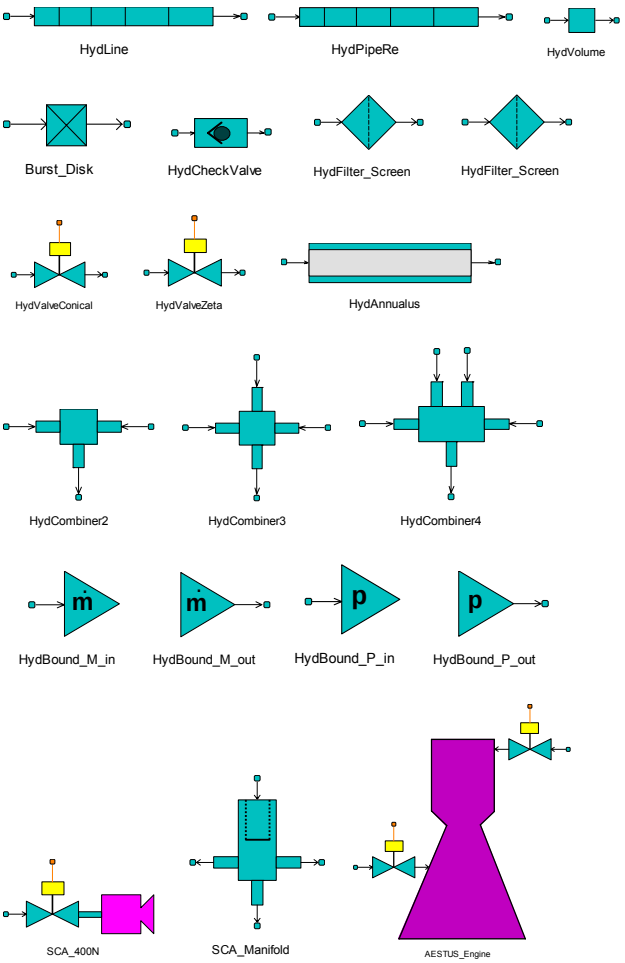


PNEUMATIK

- gas components, only forward flow
- pipes (RC) and volumes (C) include gas volume with thermodynamic properties and consideration of wall and loss calculation
- divider/combiner (RC) include gas volume with thermodynamic properties and flow calculation
- valves, orifice, filter (R) consider flow calculation
- check valves, regulators (R) consider force balance at poppet and flow calculation in dependence of poppet position
- cold gas thruster (R) consider flow calculation, performance is modelled via nozzle equation

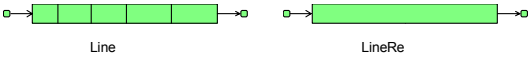


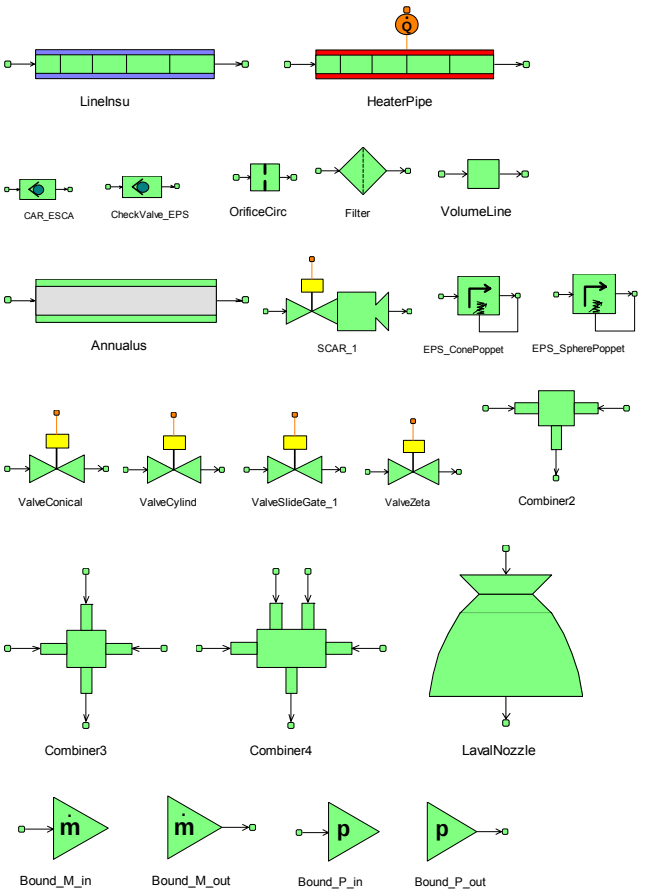


## 2. APPLICATION ON ARIANE 5 EPS

2.1 EPS STAGE MODEL - EPS propulsion system, shown in fig. 2-1, is based on a storable bi-propellant system, which is constantly pressurized by Helium. The He is stored in 2 vessels at an initial pressure of about 400 bar. The Helium flows through a 2-stage pressure regulator and will be injected into the 4 propellant tanks at 21 bar. The hypergolic propellants used are MMH as fuel and $N_2O_4$ as oxidizer, stored in 2 tanks each. These will be injected into the AESTUS engine with a mixture ratio of 2.05. Before the fuel is ignited it is used to cool the nozzle and combustion chamber. At a chamber pressure of 11 bar the engine delivers a thrust of 30 kN. The EPS propulsive stage model is a simplified representation of the used and installed stage H/W.
It has been reduced to the main functional components to characterize and adjust the behaviour and the performance of the stage for the standard GTO/SSO flight mission. The stage is composed of the following *main* components:

- 2 high pressure spherical He vessels
- 1 pyrotechnical valve PV
- mechanical 2-stage pressure regulator
- 2 latch valves LVN/M, 2 check valves CVN/M
- He venting orifice HVO
- 2 MMH fuel tanks
- 2 $N_2O_4$ oxidizer tanks

- 2 parallel flow equipments PFE for simultaneous tank depletion
- engine with 2 propellant valve assemblies PVAN/M

The operational profile of the EPS upper stage is divided into several phases. The operational phase starts with the "1st pressurization" to set the 4 propellant tanks under operational pressure of ~20 bar. After separation of the EPC stage the EPS steady state thrust phase begins. After ~800 s the LVN/M are closed and the stage works in "blow-down" mode for ~90 s until engine "shut-down".

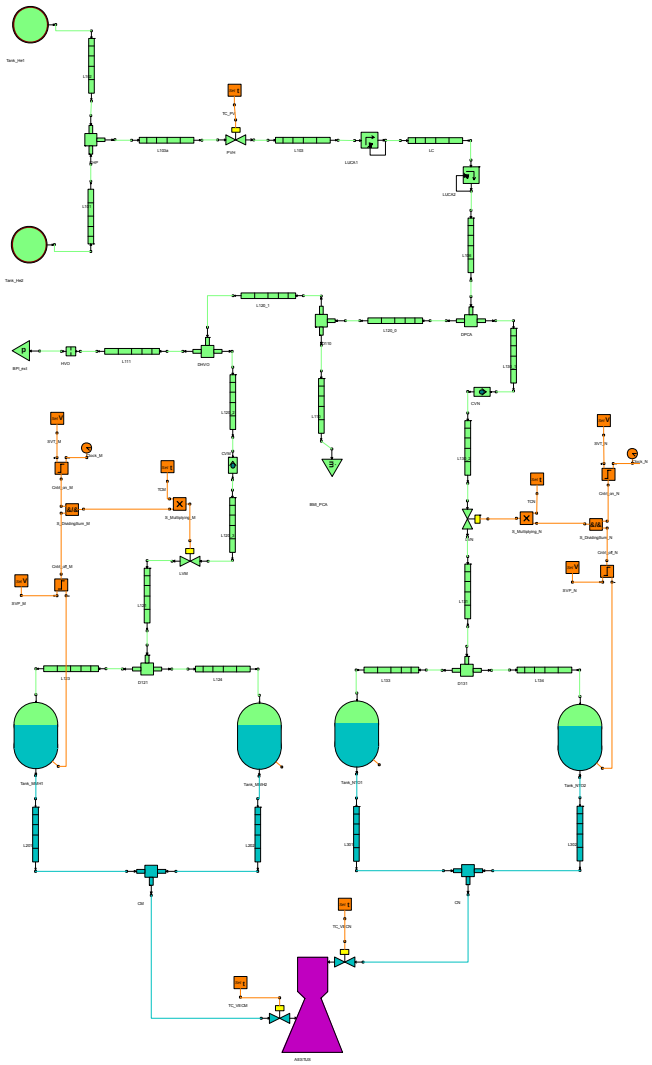

Fig. 2-1: euces schematic of EPS model

The performed flight simulation is composed of its passive flight during EAI and EPC thrust phase and the propelled phase by EPS AESTUS engine. P/L separation and stage "passivation" is not considered for the *nominal* flight prediction. The simulation results of the stage performance is generally used to adjust the A5 OBC for the individual stage specifically w.r.t. the installed H/W due to their normal scattering and deviations especially with regard on pressure regulator, valves, engine, parallel flow equipment. The exemplary flight taken into account for the comparison of stage model simulation results to flight transducer measurements is L511 to see as a 1st example for the euces COMPONENT model capability in EcosimPro kernel to such an application.

2.2 COMPONENTS - The physical formulation of the EPS components used in schematic will be briefly described hereafter for selected COMPONENTs.

Gas Tank - The physical formulation of the *gas* is basing of the mass and energy conservation. The thermodynamic state equation uses a (p, T) dependent correction factor Z to account for real gas behavior.

The rate of change of gas mass $m'$ inside the tank is given by:

$$m' = -\dot{m}_o \qquad 2.1$$

The rate of change of gas density $\rho'$ is:

$$\rho' = \frac{m'}{V} \qquad 2.2$$

The rate of change of gas pressure $p'$ can be obtained from the derivative of the state equation:

$$\rho' = \frac{\partial \rho}{\partial T} T' + \frac{\partial \rho}{\partial p} p' \qquad 2.3$$

The rate of change of gas specific enthalpy $h'$ inside the tank is given by:

$$m h' + m' h - p' V = -\dot{H}_{out} + \dot{Q} \qquad 2.4$$

$$\dot{Q} = \alpha \, S \, (T_1 - T) \qquad 2.5$$

where $\dot{Q}$ is the heat flux between vessel wall and gas. It equalizes to the heat flux to the 1st wall layer $\dot{Q}_{1,e}$. The rate of change of gas temperature $T'$ is given by:

$$h' = \frac{\partial h}{\partial T} T' + \frac{\partial h}{\partial p} p' \qquad 2.6$$

with:

$$\frac{\partial h}{\partial T} = c_p = 5191.6 \qquad 2.7$$

and

$$\frac{\partial h}{\partial p} = 0.003167 \qquad 2.8$$

The physical formulation for the tank shell is considered 1-dimensionally in spherical coordinates in radial direction which leads to per discretized volume i:

$$\rho_i \, c_i \, T_i' V_i = \dot{Q}_{i,w} - \dot{Q}_{i,e} \qquad 2.9$$

The volume wise heat flux $\dot{Q}_i$ in spherical coordinates leads to the following 2 equations for **w**est and **e**ast side:

$$\dot{Q}_{i,e} = -\frac{T_i - T_{i-1}}{\frac{b_i}{\lambda_i} + \frac{a_{i-1}}{\lambda_{i-1}}} \cdot \frac{S_{i-1}}{r^2_{\,i-\frac{1}{2}}} \qquad 2.10$$

$$\dot{Q}_{i,w} = -\frac{T_{i+1} - T_i}{\frac{b_{i+1}}{\lambda_{i+1}} + \frac{a_i}{\lambda_i}} \cdot \frac{S_{i+1}}{r^2_{\,i+\frac{1}{2}}} \qquad 2.11$$

with

$$a_i = \frac{1}{r_i} - \frac{1}{r_{i+\frac{1}{2}}} \qquad b_i = \frac{1}{r_{i-\frac{1}{2}}} - \frac{1}{r_i} \qquad 2.12$$

$$r_{i\pm\frac{1}{2}} = r_i \pm \frac{\Delta r_i}{2} \qquad 2.13$$

$$V_i = \frac{4}{3}\pi \cdot \left( r^3_{\,i+\frac{1}{2}} - r^3_{\,i-\frac{1}{2}} \right) \qquad 2.14$$

$$S_{i\pm1} = 4\pi \cdot r^2_{\,i\pm\frac{1}{2}} \qquad 2.15$$

The heat transfer coefficient $\alpha$ between internal wall and gas is set to 50 W/m$^2$/K which fits well to the comparison.

Gas Line, Divider, Combiner - The physical formulation for *gas* part of these COMPONENTs is identical to the one presented for the Gas Tank, besides that the difference PORT numbers which have to be considered in the mass and energy balance, respectively. For the Line a heat transfer correlation by Nu-number is used accounting for laminar and turbulent flow conditions inside the tube:

$$Nu = \sqrt[3]{3.66^3 + 1.61^3 \,\mathrm{Re}\,\mathrm{Pr}\,\frac{d}{l}} \qquad \mathrm{Re} < 2300 \qquad 2.16$$

$$Nu = 0.0214\,\mathrm{Re}^{0.8}\,\mathrm{Pr}^{0.4}\left(1 + \left(\frac{d}{l}\right)^{\frac{2}{3}}\right)\left(\frac{\mathrm{Pr}}{\mathrm{Pr}_w}\right)^{0.11} \qquad 2.17$$

$$\mathrm{Re} \geq 2300$$

The conservation of momentum is expressed in steady state formulation for the in- and outflow rate as follows:

$$p_i - p = \frac{\varsigma}{2}\frac{\dot{m}_i^2}{2\rho A^2} \qquad 2.18a$$

$$p - p_o = \frac{\varsigma}{2}\frac{\dot{m}_o^2}{2\rho A^2} \qquad 2.18b$$

The coupling to a wall is not considered for the Divider and Combiner. The physical formulation of the Line is already published in detail, see [1].

2-Stage Regulator, Latch Valve, Check Valve - The physical formulation of these COMPONENTs is already published in detail, see [1].

Propellant Tank - The physical formulation of the *ullage gas* is basing on the mass and energy conservation for a gas mixture.

The conservation of gas $m_g$ and vapor $m_v$ mass inside the tank ullage is given by:

$$m_g' = \dot{m}_i \qquad 2.19$$

$$m_v' = \dot{m}_{ev} \qquad 2.20$$

The conservation of total mass $m$ and mass $\xi$ fraction is:

$$m_g' = (1-\xi)\,m' - \xi' m \qquad 2.21$$

$$m_v' = \xi\, m' + \xi' m \qquad 2.22$$

The rate of change of gas $p_g'$ and vapour pressure $p_v'$ can be obtained from the derivative of the state equation:

$$\rho_g' = \frac{\partial \rho_g}{\partial T} T' + \frac{\partial \rho_g}{\partial p_g} p_g' \qquad 2.23$$

$$\rho_v' = \frac{\partial \rho_v}{\partial T} T' + \frac{\partial \rho_v}{\partial p_v} p_v' \qquad 2.24$$

The derivative of the total pressure $p'$ is the sum of the derivative of partial pressures:

$$p' = p_g' + p_v' \qquad 2.25$$

The rate of change of gas $\rho_g'$ and vapour density $\rho_v'$ can be obtained from:

$$m_g' = \rho_g V_u' + \rho_g' V_u \qquad 2.26$$

$$m_v' = \rho_v V_u' + \rho_v' V_u \qquad 2.27$$

The rate of change of ullage volume $V_u'$ is equal to the inverse rate of change of liquid volume $-V_l'$.
The averaged density $\rho$ is the sum of gas and vapor density:

$$\rho = \left( \frac{\rho_g}{\tilde{M}_g} + \frac{\rho_v}{\tilde{M}_v} \right) \tilde{M} \qquad 2.28$$

The rate of change of gas specific enthalpy $h'$ inside the ullage is given by:

$$m\,h' + m'h - p'V_u = \dot{H}_{in} + \dot{H}_{ev} - \dot{Q}_{ph} + \dot{Q}_{w,u} \qquad 2.29$$

$$\dot{Q}_{w,u} = \alpha_{w,u}\, S_{w,u} \left( T_{w,u} - T_{jet} \right) \qquad 2.30$$

where $\dot{Q}_{w,u}$ is the heat flux between tank wall and ullage and $\dot{Q}_{ph}$ is the heat flux between liquid phase interface and ullage. The heat transfer coefficient $\alpha_{w,u}$ is dependent on the flow conditions within ullage i.e. natural or forced convection. For forced convection the following Nusselt number is used for laminar

$$Nu_{lam} = 0.664 \cdot \sqrt{\mathrm{Re}} \cdot \sqrt[3]{\mathrm{Pr}} \qquad 2.31$$

and turbulent flow

$$Nu_{turb} = \frac{0.037 \cdot \mathrm{Re}^{0.8} \cdot \mathrm{Pr}}{1 + 2.443 \cdot \mathrm{Re}^{-0.1} \left( \mathrm{Pr}^{2/3} - 1 \right)} \qquad 2.32$$

Quadratic superposition of the above equations of laminar and turbulent convection leads to:

$$Nu_{forced} = \sqrt{Nu_{lam}^2 + Nu_{turb}^2} \qquad 2.33$$

For free convection the following Nusselt number is used for $Ra$ number > $10^3$:

$$Nu_{free} = 0.13 \cdot (Gr \cdot \mathrm{Pr})^{\frac{1}{3}} \qquad 2.34$$

As characteristic length $l$ for the ullage or liquid part of a propellant tank the respective volume $V$ is used by:

$$l = 2 \left( \frac{3V}{4\pi} \right)^{\frac{1}{3}} \qquad 2.35$$

A distinction has to be introduced in dependence to the temperatures and pressurization mass flow for the time-dependent Nusselt number. The superposition of natural and forced convection leads to 3 cases.

a) $\left( \dot{m}_i < 0 \wedge T_{w,u} < T \vee \dot{m}_i > 0 \wedge T_{w,u} > T \right)$:

$$Nu = \sqrt[3]{Nu_{free}^3 + Nu_{forced}^3} \qquad 2.36$$

b) $\left( \dot{m}_i < 0 \wedge T_{w,u} > T \vee \dot{m}_i > 0 \wedge T_{w,u} < T \right)$:

$$Nu = \sqrt[3]{Nu_{free}^3 - Nu_{forced}^3} \qquad 2.37$$

c) others:

$$Nu = Nu_{free} \qquad 2.38$$

The heat transfer coefficient $\alpha_{ph}$ uses for forced convection $\dot{m}_i > 0$ the equations 2.31 to 2.33. For free convection the following Nusselt number correlations are applied for $Ra$ number > $10^3$ in dependence of $T_{ph}$:

a) $\left( T > T_{ph} \right)$:

$$Nu_{free} = 0.6 \cdot \left( Gr \cdot \mathrm{Pr} \cdot f\left( \mathrm{Pr} \right) \right)^{0.2} \qquad 2.39$$

b) $\left( T < T_{ph} \right)$:

1) $\left( Ra \cdot f\left( \mathrm{Pr} \right) < 7 \cdot 10^4 \right)$:

$$Nu_{free} = 0.766 \cdot \left( Gr \cdot \mathrm{Pr} \cdot f\left( \mathrm{Pr} \right) \right)^{0.2} \qquad 2.40$$

2) $\left( Ra \cdot f\left( \mathrm{Pr} \right) \geq 7 \cdot 10^4 \right)$

$$Nu_{free} = 0.15 \cdot \left( Gr \cdot \mathrm{Pr} \cdot f\left( \mathrm{Pr} \right) \right)^{0.333} \qquad 2.41$$

The rate of change of ullage temperature $T'$ can be derived from the derivative of total specific enthalpy $h'$:

$$h' = \left( 1 - \xi \right) h_g' + \xi\, h_v' + \xi' \left( h_v - h_g \right) \qquad 2.42$$

$$h_g' = \frac{\partial h_g}{\partial T} T' + \frac{\partial h_g}{\partial p_g} p_g' \qquad 2.43$$

$$h_v' = \frac{\partial h_v}{\partial T} T' + \frac{\partial h_v}{\partial p_v} p_v' \qquad 2.44$$

The evaporated mass flow $\dot{m}_{ev}$ from the liquid phase interface of the propellant into the ullage is expressed by [3]:

$$\dot{m}_{ev} = \rho_v(p,T)\, \beta\, S_{ph} \cdot \ln \frac{1 - \psi}{1 - \psi_{s,ph}} \qquad 2.45$$

with $\beta$ as mass transfer coefficient [4]:

$$\beta = \frac{\alpha}{\rho c_p} Le^{-\frac{2}{3}} \qquad 2.46$$

The Le-number is defined as follows:

$$Le = \frac{Sc}{\mathrm{Pr}} = \frac{\lambda}{\rho c_p\, \delta} \qquad 2.47$$

where $\delta$ is the binary diffusion coefficient of which a theoretical model is published in detail in [5]. As a result for the $\dot{H}_{ev}$ follows therefore:

$$\dot{H}_{ev} = \dot{m}_{ev} h_v \qquad 2.48$$

The heat transfer induced by the jet of injected pressurization gas plays a relevant role for prediction accuracy. The model assumes to calculate the jet temperature $T_{jet}$ as a weighted value of the jet injection and the ullage temperature.

$$T_{jet} = \frac{T}{1+\frac{w_i}{w^*}} \cdot \left(1+\frac{w_i}{w^*}\frac{T_i}{T}\right) \qquad 2.49$$

where $w^*$ is a const. The inlet velocity $w_{in}$ is calculated from a geometrical consideration of the jet form:

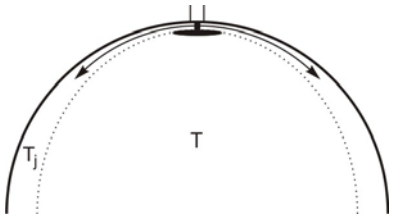


Fig. 2-2: Illustration of He injection form [6]

$$w_i = \frac{\dot{m}_i}{\rho_i \, \pi \, l \, 0.02 \, h_u} \qquad 2.50$$

The physical formulation of the *liquid pool* is basing on the mass and energy conservation.

The rate of change of *liquid* mass $m'$ inside the propellant tank is given by:

$$m_l' = -\dot{m}_{pro} - \dot{m}_{ev} \qquad 2.51$$

The rate of change of liquid density $\rho_l'$ can be obtained from:

$$m_l' = \rho_l V_l' + \rho_l' V_l \qquad 2.52$$

The rate of change of pressure $p'$ is obtained from the derivative of the ullage pressure:

$$\rho_l' = \frac{\partial \rho_l}{\partial T_l} T_l' \qquad 2.53$$

The rate of change of liquid specific enthalpy $h_l'$ inside the tank is given by:

$$m_l h_l' + m_l' h_l - p' V_l = -\dot{H}_{pro} - \dot{H}_{ev} + \dot{Q}_{ph} + \dot{Q}_{w,l} \qquad 2.54$$

$$\dot{Q}_{w,l} = \alpha_{w,l} \, S_{w,l} \left(T_{w,l} - T_l\right) \qquad 2.55$$

where $\dot{Q}_{w,l}$ is the heat flux between tank wall and liquid. The heat transfer coefficient $\alpha_{w,l}$ is dependent on the flow conditions within the liquid whereby only natural convection is considered acc. to equ. 2.34. The rate of change of liquid temperature $T_l'$ is given by:

$$h_l' = c_{p,l} T_l' \qquad 2.56$$

with:

$$c_{p,NTO} = 1581 \left[\frac{J}{kg\,K}\right] \qquad 2.57$$

$$c_{p,MMH} = 2885.2 \left[\frac{J}{kg\,K}\right] \qquad 2.58$$

The conservation of energy is set for both tank compartments - ullage (u) / liquid (l) - separately. On each tank wall part a time-dependent heat load $\dot{Q}_s$ can be applied.

$$\rho_s \, c_s \, T_s' \, V_s = \dot{Q}_s - \dot{Q}_w \qquad 2.59$$

The determination of the *filling level* $h$ is dependent on the propellant filling rate and the tank geometric shape. In this case the tank is composed of 2 half-spheres with a cylindrical intersection. The total volume $V_t$ is:

$$V_t = V_{cyl} + 2V_{hsp} = \pi R^2 H + \frac{4}{3}\pi R^3 \qquad 2.60$$

The pressure dependent stretching rate of the propellant tank is considered via the variation of the cylindrical section length $H_p$ of the tank. The modified volume $V_p$ is defined as:

$$V_p = V_t\left(1+\chi\left(p-p_a\right)\right) \qquad 2.61$$

With the volume definitions a cubic equation is obtained from which the ullage/liquid levels can be calculated as one of the real squares:

$$z^3 - 3rz^2 + 3\frac{V}{\pi} = 0 \qquad 2.62$$

Finding a solution of the cubic equation is described in [5]. Three cases have to be distinguished to evaluate the filling high $h$ in dependence of the liquid volume $V$:

a) $V_p > V \geq \left(V_{hsp1} + V_{cyl}\right)$
b) $\left(V_{hsp1} + V_{cyl}\right) > V \geq V_{hsp1}$
c) $V_{hsp1} > V$

Exemplarily case a) is presented hereafter. The solution of the cubic eq. (2.48) is:

$$z = R\left\{1 + 2\cos\left(\frac{1}{3}\arccos\left(1-\frac{V_p - V}{V_{hsp}}\right)+\frac{4}{3}\pi\right)\right\} \qquad 2.63$$

The filling level $h$ is:

$$h = 2R + H - z \qquad 2.64$$

The phase I/F surface $A$ is:

$$A = \pi z(2R - z) \qquad 2.65$$

and the wall surface $S$ in contact with the liquid:

$$S = 2\pi R(2R + H - z) \qquad 2.66$$

Liquid Line, Divider, Combiner - The physical formulation for *liquid* part of these COMPONENTs is identical to the one presented for the Gas besides the resulting simplifications for the formulation of conservation of mass and energy that liquid is treated here as non-compressible medium. The conservation of momentum accounts additionally for the hydrostatic height.

AESTUS Engine - The physical formulation of the *engine* COMPONENT is basically expressed by 2 simple correlations for the AESTUS steady state conditions. The chamber pressure $p_c$ is:

$$p_c = c \cdot \dot{m}_{tot} \qquad 2.67$$

with

$$\dot{m}_{tot} = \dot{m}_{fu} + \dot{m}_{ox} \qquad 2.68$$

The specific impulse $I_{sp}$ is expressed by:

$$I_{sp} = I_{sp,o} + \frac{\partial I_{sp}}{\partial p_c}(p_c - 10.58) \qquad 2.69$$

The thrust $F$ is:

$$F = g_o \dot{m}_{tot} I_{sp} \qquad 2.70$$

The engine steady state mixture ratio $\Theta$ is:

$$\Theta = \frac{\dot{m}_{ox}}{\dot{m}_{fu}} = 2.05 \qquad 2.71$$

The conservation of momentum is expressed for the fuel and oxidizer side:

$$p_{fu,I/F} - p_c = \varsigma_{fu} \frac{\dot{m}_{fu}^2}{2\rho_{fu} A_{ref}^2} \qquad 2.72$$

$$p_{ox,I/F} - p_c = \varsigma_{ox} \frac{\dot{m}_{ox}^2}{2\rho_{ox} A_{ref}^2} \qquad 2.73$$

2.2 COMPARISON AND VERIFICATION FOR EPS STAGE MODEL - The validation has been performed by proving each operational phase of the stage step by step [6]. For every phase the simulation has been analyzed and compared to flight data sets. Observed differences between the simulation and transducer data have been adapted by adjustment of relevant component parameters or physical model formulation enhancements.

1st Pressurization Phase - The pressure regulator model formulation is based on the dynamic formulation for the poppet force balance to consider its rapid movements during initial phases according to Newton's principle for the associated forces, as induced by springs, pressures and mass inertias. Tab. 2-1 shows the regulator parameters after adjustment to flight measurements. This set of parameters corresponds to the 97% values of the given set by the regulator supplier. The difference can be explained by an existing vibration level during stage flight. Additionally, the introduction of a jet heat transfer model inside the propellant tanks was necessary to account for correct Helium gas mass consumption and LVN/M closing time event.

| Value | Stage I | Stage II |
|---|---|---|
| $c_{s,eff}$, N/mm | 747 | 94 |
| $F_{s0,eff}$, N | 717 | 900 |
| $c_D$ | 0.3 | 0.64 |
| μ, Pa s | 2000 | 1000 |

Tab. 2-1: Adjusted parameter set of pressure regulator

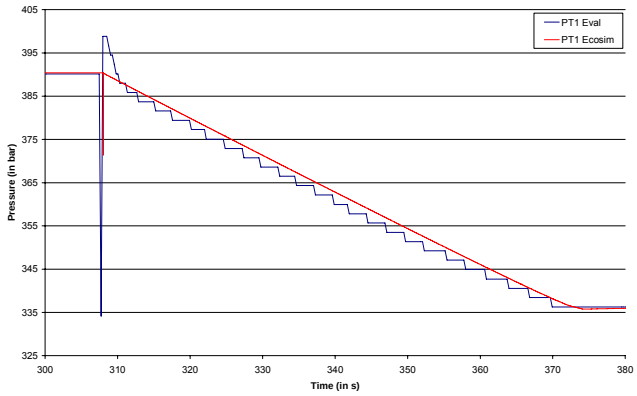


Fig. 2-3: PT1 high pressure

Fig. 2-3 presents the comparison for the high pressure PT1. The pressurization stops exactly at the time of 374s as the measured transducer value.

Fig. 2-4 displays the slope of the regulator intermediate chamber pressure PT23. The lock-up pressure is hit exactly at time and value, but the 1st pressure peak is too high. This point could not be suppressed with any kind of parameter set.

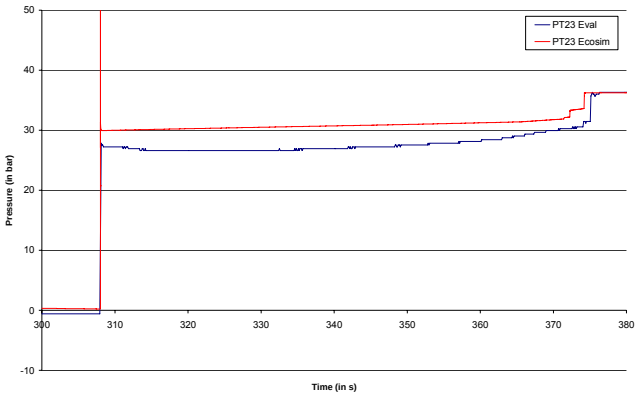


Fig. 2-4: PT23 intermediate chamber pressure

Fig 2-5 shows the pressure slope of the regulated PT3. The lock-up pressure obtains the same value as the measured one. The simulated pressure curve fits well the measured one.

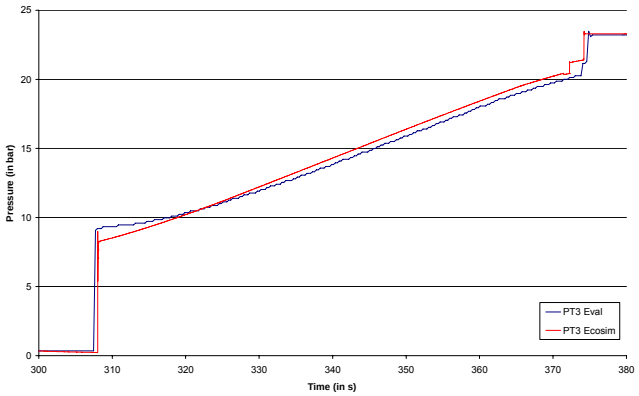


Fig. 2-5: PT3 regulated pressure

Standby Phase - The standby phase starts with the end of the 1st pressurization at 375s and ends with opening of the engine main valves VECN/M at 585s.
During the standby phase, as indicated by name, all valves are closed and no Helium or propellant flow occurs.

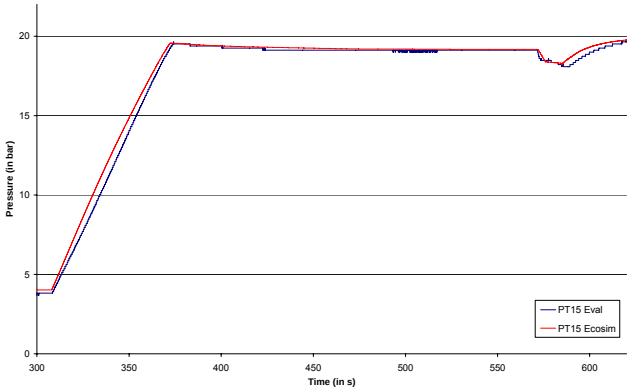


Fig. 2-6: PT15 pressure in NTO tank

Fig. 2-6 and 2-7 display the pressure slopes of the NTO and MMH tanks during this phase. As expected the observed differences between the measurement and simulation are acceptable.
The pressure curve of the NTO tank, Fig. 2-6, the pressure decreases slightly more in comparison to the measurement.

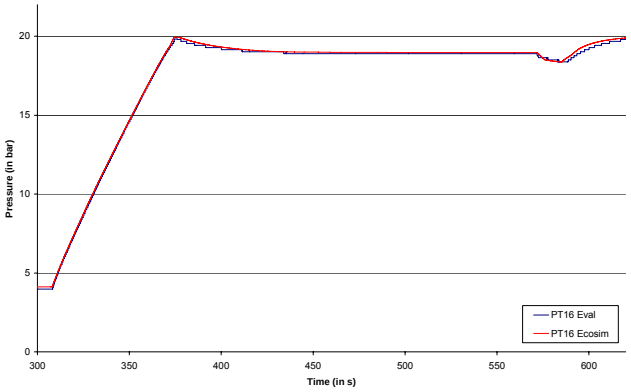


Fig. 2-7: PT16 pressure in MMH tank

The pressure of the MMH tank, Fig. 2-7, the pressure decreases perfectly to the value before the LVM opens at 584s. But the slope of the simulation is marginal higher than the measured one.
The small pressure decrease at ~580 s is due to EPC/EPS separation and comes along with a sudden decrease in axial acceleration which induces sloshing of the propellant. This leads to a bigger contact surface between ullage and propellant and yields to an increased heat transfer. Consequently, the ullage temperature decreases by breaking up the stratification, coupled with condensation of propellant vapor and pressure decrease. This effect has been considered by a mission time-dependent factor on the relevant heat transfer. Its maximum value is 10 which seem physically reasonable. There is still a difference between simulation and measurement after engine ignition at the beginning of the "pressure recovery phase" at ~580 s.

Thrust Phase - The steady state thrust phase is the operational phase of the main propulsion system where the engine is firing and the whole system is in operation. For this phase following properties have to be compared: *thrust, propellant mass flows, mixture ratio, propellant residuals, combustion chamber pressure, tank pressures, ignition/shut-down box, helium budget* and *propellant budget*. The needed and performed investigations for the adjustment of parameters were quite intensive.

A step by step approach was chosen, because all the components of the propulsion system are interdependent with each other. The accuracy of the transducers was taken into consideration and finally, the main improvement was made on the regulator and engine model.

- The regulator model has been enlarged by introducing of the temperature effect on the Young's modulus by the secondary spring which is submerged into the He flow. In sum, it reduces the

overall spring stiffness $c_{sp}$, because it counteracts to the main spring. The discharge coefficient $c_d$ of the main regulator orifice has been now formulated linear dependent on the poppet stroke $x$.

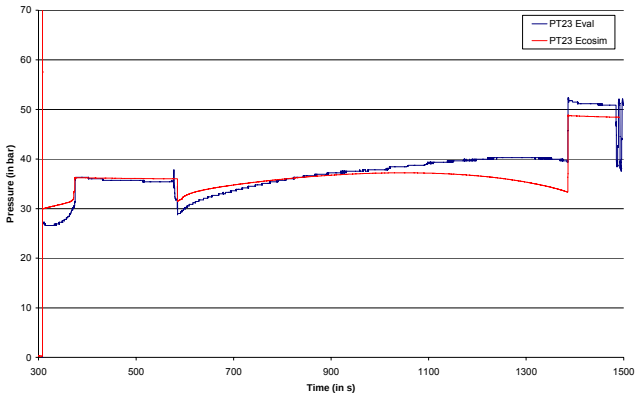


Fig. 2-8 PT23 intermediate chamber pressure

In Fig. 2-8 the intermediate chamber pressure of the regulator is displayed. The lock-up value after the 1st pressurization is well achieved, but the slope in the steady state phase differs from the measured one. There are some reasons which could lead to those differences mainly the model formulation seems too rough.

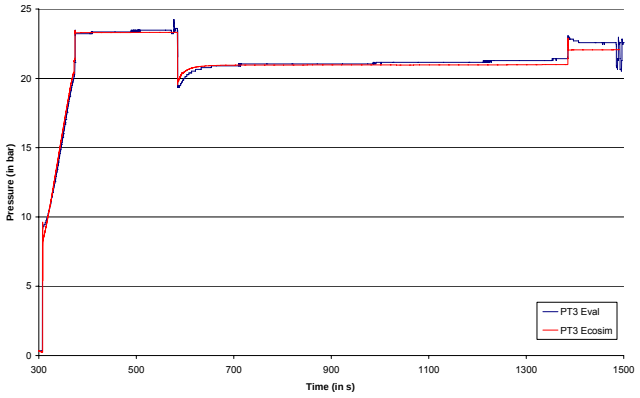


Fig. 2-9: PT3 regulated pressure

Fig. 2-9 shows the pressure slope of the regulator outlet pressure. The slope fits quite well until the final lock-up at the end of the thrust phase. The difference in the lock-up pressure is about 2% less than that for the measured value. The difference is related to the behavior of the pressure in front of the 2nd stage, i.e. the pressure PT23.

In Fig. 2-10 the pressure in the Helium tanks is shown. The curve of the model simulation fit well with the flight measurement under consideration of the transducer accuracy of 6 bar. A deviation can be remarked during the thrust phase which may be linked to a stratified temperature profile inside the tanks or uncertainties in the consideration of the external heat loads.
The Helium budget fits also well to the flight evaluation result where the residual Helium is determined to 8 kg while the simulation turns out 8.3 kg which is a deviation w.r.t. the initially loaded mass of < 1%.

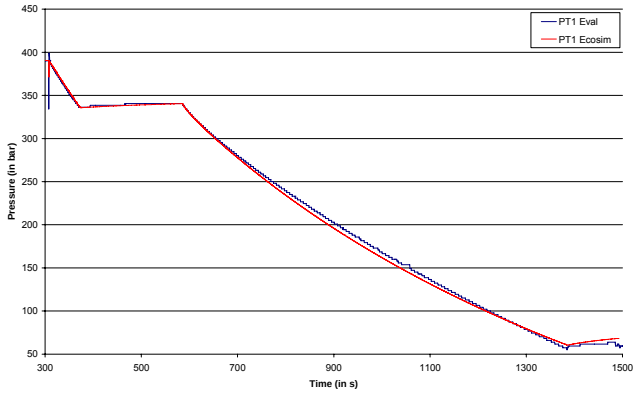


Fig. 2-10: PT1 pressure in Helium tanks

In Fig. 2-11 and 2-12 the pressure inside the propellant tanks are presented. The curves of the model simulation fit almost perfectly with the flight measurement.

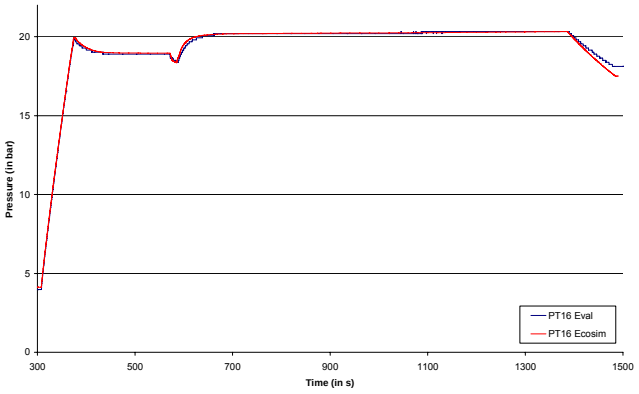


Fig. 2-11 PT16 pressure in MMH tank

The next point is the propellant mass flow rates and the engine chamber pressure and mixture ratio.

- The engine model was corrected w.r.t. a faulty chosen reference temperature for the MMH density $\rho_{fu}$ of the engine loss coefficient $\varsigma_{fu}$.

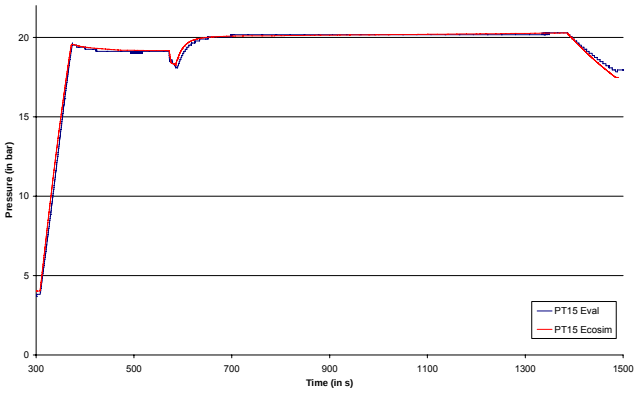


Fig. 2-12: PT15 pressure in NTO tank

The combustion chamber pressure is presented in Fig. 2-13. The slope is constantly a little below the measured one. Due to the fact that the difference is only 0.7 % it is within the accuracy of the chamber pressure transducer and therefore acceptable.

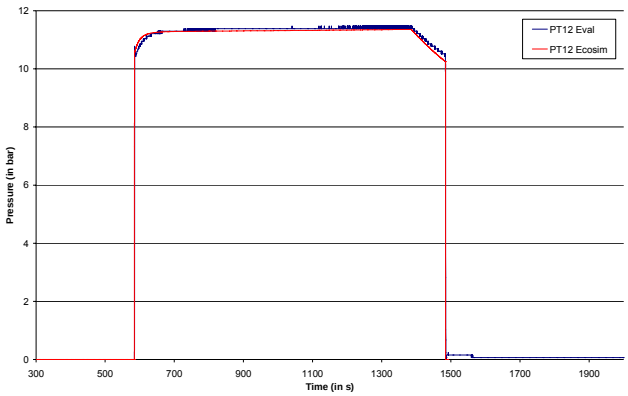


Fig. 2-13: PT12 pressure in combustion chamber

Fig. 2-14 presents the thrust profile. The simulation fits very well and the difference to the measurement is maximal 0.6 %. It has to be mentioned that the thrust is a value which is not measured directly in flight and is calculated with eq. (2-56) which was derived from engine hot firing tests.

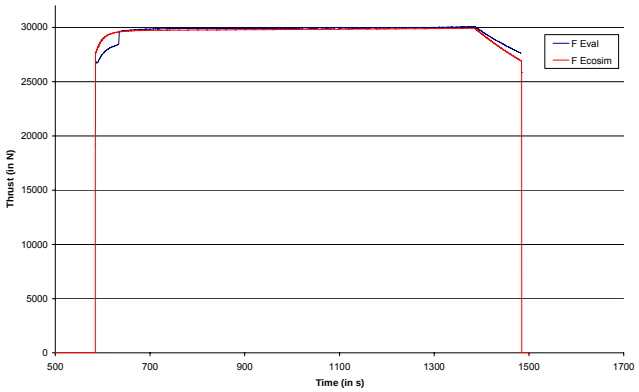


Fig. 2-14: Thrust

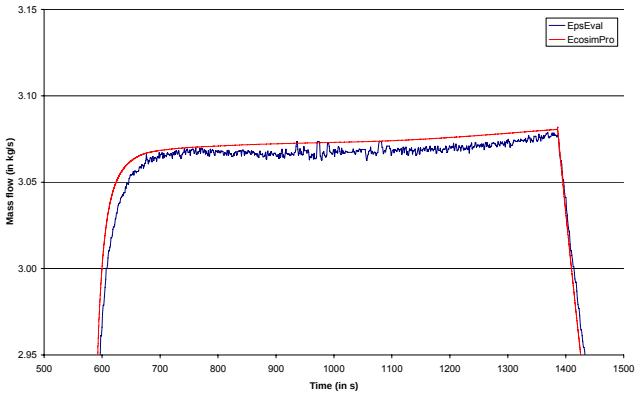


Fig. 2-15: Total mass flow MMH

Fig. 2-15 displays the mass flow of the MMH into the engine. It can be seen that the mass flow is only marginal higher than the flight evaluated one. The difference is < 0.2 % in average and therefore negligible.

Fig. 2-16 presents the total mass flow of the NTO into the engine. The difference is about 0.8 % in average, and therefore acceptable. The mass flow rate of NTO is in opposite to MMH lower than the measured one.

For both mass flow rates it has to be mentioned that the flight evaluated mass flows are indirectly measured by the differential pressure at the PFE orifices and the propellant density calculated with the measured temperature. Consequently, the simulation results are within the obtained accuracy. The accuracy is almost higher as can be derived from the two figures above. This can be explained with the AESTUS and EPS development details and cannot be explained here.

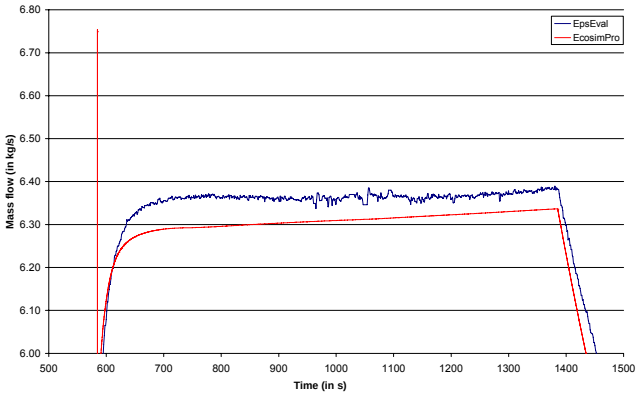


Fig. 2-16: Total mass flow NTO

Fig. 2-17 presents the mixture ratio. It can be seen that the mixture ratio of the simulation is below the measured one. The difference is 1 % in average which is basically small, but it is smaller. In comparison to the EPSSIM simulation it shows almost exactly the same result which approved the euces EPS model.

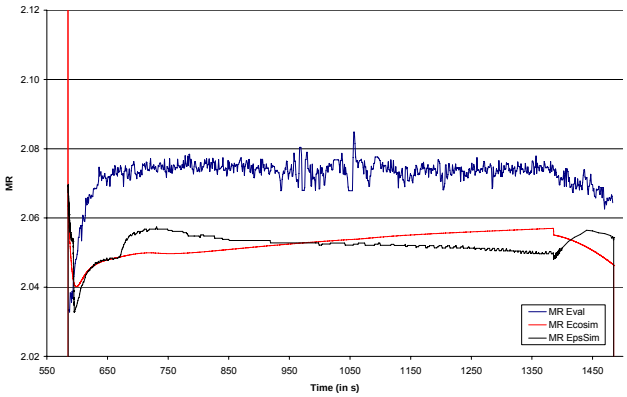


Fig. 2-17: Mixture ratio incl. EPSSIM result

## CONCLUSION

The ARIANE 5 EPS stage model shows as a propulsion system example again the power and possibilities of EcosimPro object-oriented S/W approach and the physical modeling approach of euces libraries. A well adjusted set of model parameters for the EPS could also be achieved w.r.t. the flight measurement data delivered by AS. A next step at Astrium will be to set up a full ESC-A functional stage model and to perform flight analysis simulations and to compare those to ESC-A flight measurement data. Besides propulsion system model set-up and simulation also thermal and environmental analysis tasks can be fulfilled by euces library components due to their generality in formulation and application.

## ACKNOWLEDGMENT

The euces Project Part II is funded by BMBF (federal ministry of education and science) with account no. 50RL0620 and is performed at EADS Astrium GmbH, Bremen.

## REFERENCES

1. Isselhorst, A; "euces: european cryogenic engineering software tool, AIAA paper, no. 06-6729, Keystone Col., 21-24 Aug. 2006"
2. Isselhorst, A; "euces Part I, Study on numerical Modelling and Simulation of Launcher Stages for propelled and non propelled Flight Phases, BMBF Final Report, account no. 50JR0503, Jan. 2006"
3. VDI-Gesellschaft Verfahrenstechnik und Chemie-ingenieurwesen (Herausgeber), "VDI-Wärmeatlas, Band 8. Springer-Verlag, Berlin Heidelberg,1997“
4. Stephan, K., "Wärmeübergang beim Kondensieren und beim Sieden. Springer-Verlag, Berlin, 1988."
5. Bird, B. et. al., "Transport Phenomena. New York - London, John Wiley & Sons, 1960”
6. Rackemann, N; "Validation of the EcosimPro Model for the stage simulation of the Ariane 5 upper stage EPS, Diploma Thesis, Technical University Berlin, 13. Jul. 2007 "
7. EcosimPro; "A Professional Dynamic Modeling and Simulation Tool for Industrial Applications, v3.4.2, EAI, Spain, 2005, www.ecosimpro.com"

## NOMENCLATURE

*Latin letters*

| | | |
|---|---|---|
| $A$ | cross section | m² |
| $c_D$ | discharge coefficient | |
| $c_p$ | specific heat capacity at const. pressure | J/kg/K |
| $c_{sp}$ | spring stiffness | N/m |
| $d$ | diameter | m |
| $F$ | thrust | N |
| $g$ | gravity acceleration | m/s² |
| $h$ | height | m |
| $h$ | specific enthalpy | J/kg |
| $H$ | height | m |
| $I_{sp}$ | impulse | s |
| $l$ | characteristic length | m |
| $L$ | length | m |
| $Le$ | Lewis number | |
| $m$ | mass | kg |
| $\dot{m}$ | mass flow rate | kg/s |
| $\tilde{M}$ | molar mass | kmol/m³ |
| $Nu$ | Nusselt number | |
| $p$ | pressure | Pa |
| $\mathrm{Pr}$ | Prandtl number | |
| $r$ | radius | m |
| $\dot{Q}$ | heat flux | W |
| $R$ | radius | m |
| $R$ | specific gas constant | J/kg/K |
| $Re$ | Reynolds number | |
| $S$ | surface | m² |
| $Sc$ | Schmidt number | |
| $t$ | time | s |
| $T$ | absolute temperature | K |
| $V$ | volume | m³ |
| $w$ | flow velocity | m/s |
| $x$ | poppet displacement | m |
| $z$ | solution of cubic equation | |
| $Z$ | compressibility factor | |
| $' = \partial / \partial t$ | time derivative of property | 1/s |

*Greek letters*

| | | |
|---|---|---|
| $\alpha$ | heat transfer coefficient | W/m²/K |
| $\beta$ | isothermal compressibility | 1/K |
| $\delta$ | Binary diffusion coefficient | m²/s |
| $\eta$ | dynamic viscosity | Pa s |
| $\lambda$ | heat conductivity | W/m/K |
| $\varsigma$ | loss coefficient | |
| $\psi$ | molar fraction | |
| $\rho$ | density | kg/m³ |
| $\xi$ | mass fraction | |
| $\pi$ | ratio of circumference to diameter of circle | |

*Indices*

| | |
|---|---|
| $a$ | external |
| $c$ | combustion chamber |
| $cyl$ | cylinder |
| $e$ | east |
| $fu$ | fuel |
| $g$ | gas |
| $hsp$ | half sphere |
| $i$ | inlet |
| $l$ | liquid |
| $o$ | outlet |
| $ox$ | oxidizer |
| $p$ | pressure corrected |
| $ph$ | phase I/F |
| $s$ | solid |

| | |
|---|---|
| *t* | tank |
| *tot* | total |
| *u* | ullage |
| *v* | vapor |
| *w* | wall |
| *w* | west |

## DEFINITIONS, ACRONYMS, ABBREVIATIONS

| | |
|---|---|
| A5 | **A**riane **5** Launcher |
| BMBF | **B**undes**m**inistierium für **B**ildung und **F**orschung |
| C | **C**apacitance |
| CVN/M | **C**heck **V**alve **N**TO**/M**MH |
| EAI | **E**mpresarios **A**grupados **I**nternational, Madrid |
| EADS | **E**uropean **A**eronautic and **D**efense **S**ystems |
| EL | **E**cosimPro **L**anguage |
| EPC | **E**tage **P**rincipal **C**ryotechnique |
| EPS | **E**tage **P**ropulsive **S**tockable |
| EpsSim | currently used Fortran code for EPS prediction |
| ESA | **E**uropean **S**pace **A**gency |
| ESC | **E**tage **S**upérieur **C**ryotechnique |
| euces | european cryogenic engineering software |
| GTO | **G**eostationary **E**arth **O**rbit |
| $HFE_{7000}$ | 1-methoxyheptafluoropropane |
| HVO | **H**elium **V**enting **O**rifice |
| H/W | **H**ard**w**are |
| I/F | **I**nter**f**ace |
| L511 | Ariane 5 **L**aunch **511** |
| LVN/M | **L**atch **V**alve **N**TO**/M**MH |
| MMH | **M**ono **M**ethyl **H**ydrazine |
| MR | **M**ixture **R**atio |
| NGLN | **N**ew **G**eneration **L**aunch **V**ehicles |
| NTO | **N**itrogen **T**etr**o**xide |
| OBC | **O**n **B**oard **C**omputer |
| PFE | **P**arallel **F**low **E**quipment |
| P/L | **P**ay**l**oad |
| PV | **P**yro **V**alve |
| PVA | **P**ropellant **V**alve **A**ssembly |
| R | **R**esistance |
| RC | **R**esistance **C**apacitance |
| SSO | **S**un **S**ynchronic **O**rbit |
| S/W | **S**oft**w**are |
| w.r.t. | **w**ith **r**espect **t**o |